

REPORT DOCUMENTATION PAGE				Form Approved OMB No. 0704-0188	
<p>Public reporting burden for this collection of information is estimated to average 1 hour per response, including the time for reviewing instructions, searching existing data sources, gathering and maintaining the data needed, and completing and reviewing this collection of information. Send comments regarding this burden estimate or any other aspect of this collection of information, including suggestions for reducing this burden to Department of Defense, Washington Headquarters Services, Directorate for Information Operations and Reports (0704-0188), 1215 Jefferson Davis Highway, Suite 1204, Arlington, VA 22202-4302. Respondents should be aware that notwithstanding any other provision of law, no person shall be subject to any penalty for failing to comply with a collection of information if it does not display a currently valid OMB control number. PLEASE DO NOT RETURN YOUR FORM TO THE ABOVE ADDRESS.</p>					
1. REPORT DATE (DD-MM-YYYY) May 2013		2. REPORT TYPE Technical Paper		3. DATES COVERED (From - To) May 2013-June 2013	
4. TITLE AND SUBTITLE A 3D Unstructured Mesh Euler Solver Based on the Fourth-Order CESE Method				5a. CONTRACT NUMBER In-House	
				5b. GRANT NUMBER	
				5c. PROGRAM ELEMENT NUMBER	
6. AUTHOR(S) Bilyeu, David; Yu, John; Cambier, Jean-Luc				5d. PROJECT NUMBER	
				5e. TASK NUMBER	
				5f. WORK UNIT NUMBER Q0A5	
7. PERFORMING ORGANIZATION NAME(S) AND ADDRESS(ES) Air Force Research Laboratory (AFMC) AFRL/RQRS 1 Ara Drive. Edwards AFB CA 93524-7013				8. PERFORMING ORGANIZATION REPORT NO.	
9. SPONSORING / MONITORING AGENCY NAME(S) AND ADDRESS(ES) Air Force Research Laboratory (AFMC) AFRL/RQR 5 Pollux Drive Edwards AFB CA 93524-7048				10. SPONSOR/MONITOR'S ACRONYM(S)	
				11. SPONSOR/MONITOR'S REPORT NUMBER(S) AFRL-RQ-ED-TP-2013-114	
12. DISTRIBUTION / AVAILABILITY STATEMENT Distribution A: Approved for Public Release; Distribution Unlimited. PA#13285					
13. SUPPLEMENTARY NOTES Conference paper for the AIAA CFD conference, San Diego, CA, June 2013.					
14. ABSTRACT In this paper, the CESE method is extended and employed to construct a fourth-order, three-dimensional, unstructured-mesh solver for hyperbolic Partial Differential Equations (PDEs). This new CESE method retains all favorable attributes of the original second-order CESE method, including: (i) flux conservation in space and time without using a one-dimensional Riemann solver, (ii) genuinely multi-dimensional treatment without dimensional splitting (iii) the CFL constraint remains to be ≤ 1 , and (iv) the use of a compact mesh stencil involving only the immediate neighboring nodes surrounding the node where the solution is sought. Two validation cases are presented. First higher order convergence is demonstrated by the linear advection equation. Second supersonic flow over a spherical body is simulated to demonstrates the schemes ability to accurately resolve discontinuities.					
15. SUBJECT TERMS					
16. SECURITY CLASSIFICATION OF:			17. LIMITATION OF ABSTRACT SAR	18. NUMBER OF PAGES 16	19a. NAME OF RESPONSIBLE PERSON Justin Koo
a. REPORT Unclassified	b. ABSTRACT Unclassified	c. THIS PAGE Unclassified			19b. TELEPHONE NO (include area code) 661-525-5707

A 3D Unstructured Mesh Euler Solver Based on the Fourth-Order CESE Method

David L. Bilyeu ^{*1,2}, S.-T. John Yu ^{†1}, and Jean-Luc Cambier ^{‡2}

¹The Department of Mechanical and Aerospace Engineering, The Ohio State University,
Columbus, OH 43210

²Air Force Research Laboratory, Edwards Air Force Base, CA 93524

In this paper, the CESE method is extended and employed to construct a fourth-order, three-dimensional, unstructured-mesh solver for hyperbolic Partial Differential Equations (PDEs). This new CESE method retains all favorable attributes of the original second-order CESE method, including: (i) flux conservation in space and time without using a one-dimensional Riemann solver, (ii) genuinely multi-dimensional treatment without dimensional splitting (iii) the CFL constraint remains to be ≤ 1 , and (iv) the use of a compact mesh stencil involving only the immediate neighboring nodes surrounding the node where the solution is sought. Two validation cases are presented. First higher order convergence is demonstrated by the linear advection equation. Second super sonic flow over a spherical body is simulated to demonstrate the schemes ability to accurately resolve discontinuities.

I. Introduction

Previously the CESE method has been expanded to higher order for both one-dimension,^{1,2} and two-dimensions.³ In this paper we further extend the CESE method to fourth-order accuracy in three-dimensions. Similar to the original second-order CESE method, space and time are treated in a unified manner. Although the present development is fourth-order the formulation to be presented in the paper is recursive and can be straightforwardly extended to a sixth-, eighth-order or higher by including more terms in the Taylor series expansion.

What makes the CESE scheme unique is due, in part, to the unified treatment of space and time as well as how the space-time domain is discretized. In general, the space-time domain is divided into Solution Elements (SEs) and Conservation Elements (CEs). In each SE the primary unknowns and fluxes are discretized and represented by a third-order Taylor series. The CE area a series of non-overlapping regions that fill the entire domain. These elements are mechanism in which flux conservation is enforced. The numerical integration is aided by the discretized unknowns and fluxes defined in each SE. In general, CEs do not coincide with SEs. By enforcing flux conservation over each CE, a set of algebraic equations in term of the unknown and its spatial derivatives are derived. By solving the equations the solution at the next time step is calculated. As will be shown in the following sections, the time-marching calculation of the three-dimensional fourth-order CESE method is explicit.

The remainder of this paper is organized as follows. Section II presents the three-dimensional, fourth-order CESE method and is divided into the following sub-sections: (A) properties of Taylor series, (B) the calculation of the fluxes and their derivatives, (C) the calculation of the temporal derivatives of the conserved variables, (D) space-time integration for conserved variables and their even derivatives (E) central differencing approach for calculating the odd derivatives (F) outline of the numerical calculation. Section III reports the numerical results by using the new four-order CESE method. At the end of the paper, we present the concluding remarks and provide the list of the cited references.

^{*}Ph.D. Candidate of Mechanical Engineering, Email: bilyeu.4@osu.edu, AIAA Student Member.

[†]Associate Professor of Mechanical Engineering, Email: yu.274@osu.edu, AIAA Member.

[‡]Senior Aerospace Scientist, Email: jean-luc.cambier@edwards.af.mil, AIAA Member.

II. Numerical Method

A three-dimensional hyperbolic equation is cast into the following vector form:

$$\frac{\partial \mathbf{U}}{\partial t} + \frac{\partial \mathbf{F}^x}{\partial x} + \frac{\partial \mathbf{F}^y}{\partial y} + \frac{\partial \mathbf{F}^z}{\partial z} = 0 \quad (1)$$

where $\mathbf{U} = (u_1, u_2, \dots, u_m)^t$, $\mathbf{F}^{x,y,z} = (f_1^{x,y,z}, f_2^{x,y,z}, \dots, f_m^{x,y,z})^t$, and m is the number of equations in the system. Each of the equations in Eq. (1) is a divergence-free condition: $\nabla \cdot \mathbf{h}_i = 0$, where $i = 1, \dots, m$ and $\mathbf{h}_i = (f_i^x, f_i^y, f_i^z, u_i)^t$ is the space-time flux function. Here, the divergence operates in the four-dimensional Euclidean space (x, y, z, t) . Aided by Gauss' theorem, the integral form of Eq. (1) becomes

$$\oint \mathbf{h}_i(x, y, z, t) \cdot d\mathbf{s} = 0. \quad (2)$$

The CESE method is designed to integrate Eq. (2) in the space-time domain. In the numerical algorithm, space and time are treated in a unified manner.

The geometry for a three-dimensional CESE method is more difficult to visualize than the one- and two-dimensional methods because the integration is carried out in four-dimensions, three spatial and one temporal. As such the CE and SE discretization will not be shown.

II.A. The Taylor Series Expansion

A N th-order Taylor series expansion of the conserved variables u_i inside a SE can be written in the following form:

$$u_i(x, y, z, t) = \sum_{a=0}^N \sum_{b=0}^{N-a} \sum_{c=0}^{N-a-b} \sum_{d=0}^{N-a-b-c} \frac{\partial^{a+b+c+d} u_i}{\partial x^a \partial y^b \partial z^c \partial t^d} \frac{\Delta x^a}{a!} \frac{\Delta y^b}{b!} \frac{\Delta z^c}{c!} \frac{\Delta t^d}{d!} \quad (3)$$

where $\Delta x = x - x_j$, $\Delta y = y - y_j$, $\Delta z = z - z_j$, and $\Delta t = t - t^n$. The subscript j and the superscript n are respectively the spatial and temporal anchoring point. For the fourth-order CESE method a third-order Taylor expansion in space and time is employed, $N = 3$. Since the CESE scheme does not assume the symmetry property of derivatives, e.g. $\frac{\partial^2 u}{\partial x \partial y}$ and $\frac{\partial^2 u}{\partial y \partial x}$ are two distinct variables, Eq. (3) is not initially compatible with this assumption. In order to use Eq. (3) within our scheme the mixed derivatives needs to be averaged. For example

$$\frac{\partial^3 u_i}{\partial x^2 \partial z} \equiv \frac{1}{3} \left(\frac{\partial^3 u_i}{\partial x \partial x \partial z} + \frac{\partial^3 u_i}{\partial x \partial z \partial x} + \frac{\partial^3 u_i}{\partial z \partial x \partial x} \right)$$

Moreover, a derivative of u_i can also be expressed by a Taylor series expansion. All derivatives of u_i in Eq. (3) can be succinctly expressed by the following Taylor series expansion:

$$\frac{\partial^C u_i}{\partial x^I \partial y^J \partial z^K \partial t^L} = \sum_{a=0}^A \sum_{b=0}^{A-a} \sum_{c=0}^{A-a-b} \sum_{d=0}^{A-a-b-c} \frac{\partial^B u_i}{\partial x^{I+a} \partial y^{J+b} \partial z^{K+c} \partial t^{L+d}} \frac{\Delta x^a}{a!} \frac{\Delta y^b}{b!} \frac{\Delta z^c}{c!} \frac{\Delta t^d}{d!} \quad (4)$$

where $C = I + J + K + L$, $A = N - C$, and $B = C + a + b + c + d$. Obviously, the Taylor series expansion of u_i , Eq. (3), is a special case of Eq. (4) with $A = N$ and $C = 0$. Similarly, the fluxes, $f_i^{x,y,z}$, and their derivatives inside a SE are also discretized by the Taylor series expansion:

$$\frac{\partial^C f_i^{x,y,z}}{\partial x^I \partial y^J \partial z^K \partial t^L} = \sum_{a=0}^A \sum_{b=0}^{A-a} \sum_{c=0}^{A-a-b} \sum_{d=0}^{A-a-b-c} \frac{\partial^B f_i^{x,y,z}}{\partial x^{I+a} \partial y^{J+b} \partial z^{K+c} \partial t^{L+d}} \frac{\Delta x^a}{a!} \frac{\Delta y^b}{b!} \frac{\Delta z^c}{c!} \frac{\Delta t^d}{d!} \quad (5)$$

where C and B have the same definitions as that in Eq. (4). When $C = 0$, Eq. (5) is the Taylor series expansion of the flux $f_i^{x,y,z}$ itself.

The Taylor series coefficients listed in Eqs. (4) and (5) are the unknown variables that need to be calculated as part of the Higher Order CESE method.

In the following derivation it will be shown that the only independent variables are the conserved variables and their spatial derivatives. This requires that the fluxes and their derivatives as well as the temporal derivatives of the conserved variables are functions of the conserved variables and their spatial derivatives.

II.B. Flux Terms

In a previous paper,³ it was demonstrated that the flux terms and their spatial and temporal derivatives can be expressed as functions of the conserved variables. This is accomplished through the Jacobian and its derivatives or through a generalized Leibniz rule.^{4,5} In short both of these methods demonstrated this by recognizing that the flux functions and their derivatives can be written as functions of the conserved variables, and their derivatives. The Jacobian method is more generic and as such will be used to show this relationship.

Aided by the chain rule, the first derivatives of $f_i^{x,y,z}$ can be represented as

$$\frac{\partial f_i^{x,y,z}}{\partial \Psi_1} = \sum_{l=1}^m \frac{\partial f_i^{x,y,z}}{\partial u_l} \frac{\partial u_l}{\partial \Psi_1}, \quad (6)$$

where $\Psi_1 = x, y, z$, and t . On the right hand side of Eq. (6), $\partial f_i^{x,y,z} / \partial u_l$ is the Jacobian matrix, which can be easily derived from the relationship between the fluxes and the conserved quantities. For the second derivatives, we have

$$\frac{\partial^2 f_i^{x,y,z}}{\partial \Psi_1 \partial \Psi_2} = \sum_{l=1}^m \frac{\partial f_i^{x,y,z}}{\partial u_l} \frac{\partial^2 u_l}{\partial \Psi_1 \partial \Psi_2} + \sum_{l=1}^m \sum_{p=1}^m \frac{\partial^2 f_i^{x,y,z}}{\partial u_l \partial u_p} \frac{\partial u_l}{\partial \Psi_1} \frac{\partial u_p}{\partial \Psi_2}, \quad (7)$$

where

$$(\Psi_1, \Psi_2) = \begin{matrix} (x, x), (x, y), (x, z), (x, t), \\ (y, x), (y, y), (y, z), (y, t), \\ (z, x), (z, y), (z, z), (z, t), \\ \text{and } (t, t) \end{matrix}$$

The second term on the right hand side of Eq. (7), $\partial^2 f_i^{x,y,z} / \partial u_l \partial u_p$ is a $m \times m \times m$, matrix, which can be readily derived based on the governing equations. For the third derivatives, we have

$$\begin{aligned} \frac{\partial^3 f_i^{x,y,z}}{\partial \Psi_1 \partial \Psi_2 \partial \Psi_3} &= \sum_{l=1}^m \frac{\partial f_i^{x,y,z}}{\partial u_l} \frac{\partial^3 u_l}{\partial \Psi_1 \partial \Psi_2 \partial \Psi_3} + \\ &\sum_{l=1}^m \sum_{p=1}^m \frac{\partial^2 f_i^{x,y,z}}{\partial u_l \partial u_p} \left(\frac{\partial^2 u_l}{\partial \Psi_1 \partial \Psi_2} \frac{\partial u_p}{\partial \Psi_3} + \frac{\partial^2 u_l}{\partial \Psi_1 \partial \Psi_3} \frac{\partial u_p}{\partial \Psi_2} + \frac{\partial^2 u_l}{\partial \Psi_2 \partial \Psi_3} \frac{\partial u_p}{\partial \Psi_1} \right) + \\ &\sum_{l=1}^m \sum_{p=1}^m \sum_{q=1}^m \frac{\partial^3 f_i^{x,y,z}}{\partial u_l \partial u_p \partial u_q} \frac{\partial u_l}{\partial \Psi_1} \frac{\partial u_p}{\partial \Psi_2} \frac{\partial u_q}{\partial \Psi_3}, \end{aligned} \quad (8)$$

$$(\Psi_1, \Psi_2, \Psi_3) =$$

$$\begin{matrix} (x, x, x), (x, x, y), (x, x, z), (x, x, t), (x, y, x), (x, y, y), (x, y, z), (x, y, t), (x, z, x), (x, z, y), (x, z, z), (x, z, t), \\ (y, x, x), (y, x, y), (y, x, z), (y, x, t), (y, y, x), (y, y, y), (y, y, z), (y, y, t), (y, z, x), (y, z, y), (y, z, z), (y, z, t), \\ (z, x, x), (z, x, y), (z, x, z), (z, x, t), (z, y, x), (z, y, y), (z, y, z), (z, y, t), (z, z, x), (z, z, y), (z, z, z), (z, z, t), \\ (x, t, t), (y, t, t), (z, t, t), (t, t, t) \end{matrix}$$

The last term on the right hand side of Eq. (8), $\partial^3 f_i^{x,y,z} / \partial u_l \partial u_p \partial u_q$ is a $m \times m \times m \times m$ matrix, which can be readily derived based in the definition of $f_i^{x,y,z}$ as functions of u_i . Aided by Eqs. (6-8), we can relate all derivatives of $f_i^{x,y,z}$ to the derivatives of u_i .

II.C. Temporal Derivatives

As with the two-dimensional fourth-order CESE scheme³ the Cauchy-Kovalewski procedure for non-linear equations is used to relate the temporal derivatives of the conserved variables to the conserved variables and its spatial derivatives.

To begin we let the Taylor series satisfy Eq. (1) at point (j, n) ,

$$\left(\frac{\partial u_i}{\partial t}\right)_j^n = -\left(\frac{\partial f_i^x}{\partial x}\right)_j^n - \left(\frac{\partial f_i^y}{\partial y}\right)_j^n - \left(\frac{\partial f_i^z}{\partial z}\right)_j^n \quad (9)$$

Each term in the above equation is a coefficient in a Taylor series. For conciseness the super- and sub-scripts, i.e., j and n , indicating the space-time location are dropped in the following equations. Aided by Eq. (9), the second-order derivatives of u_i involving first-order time differentiation are readily available by assuming that the following algebraic equations are valid:

$$\begin{aligned} \frac{\partial^2 u_i}{\partial x \partial t} &= -\frac{\partial^2 f_i^x}{\partial x \partial x} - \frac{\partial^2 f_i^y}{\partial y \partial x} - \frac{\partial^2 f_i^z}{\partial z \partial x}, & \frac{\partial^2 u_i}{\partial y \partial t} &= -\frac{\partial^2 f_i^x}{\partial x \partial y} - \frac{\partial^2 f_i^y}{\partial y \partial y} - \frac{\partial^2 f_i^z}{\partial z \partial y}, \\ \frac{\partial^2 u_i}{\partial z \partial t} &= -\frac{\partial^2 f_i^x}{\partial x \partial z} - \frac{\partial^2 f_i^y}{\partial y \partial z} - \frac{\partial^2 f_i^z}{\partial z \partial z}, & \frac{\partial^2 u_i}{\partial t \partial t} &= -\frac{\partial^2 f_i^x}{\partial x \partial t} - \frac{\partial^2 f_i^y}{\partial y \partial t} - \frac{\partial^2 f_i^z}{\partial z \partial t} \end{aligned} \quad (10)$$

Even though the final relation in Eq. (10) has a temporal derivative on the right hand side of the equation it is still a function of spatial derivatives. As an example we look at the first term on the RHS $\frac{\partial^2 f_i^x}{\partial x \partial t}$ which can be expressed as

$$\begin{aligned} \frac{\partial^2 f_i^x}{\partial x \partial t} &= \sum_{l=1}^m \frac{\partial f_i^x}{\partial u_l} \frac{\partial^2 u_l}{\partial x \partial t} + \sum_{l=1}^m \sum_{p=1}^m \frac{\partial^2 f_i^x}{\partial u_l \partial u_p} \frac{\partial u_l}{\partial x} \frac{\partial u_p}{\partial t} \\ &= -\sum_{l=1}^m \frac{\partial f_i^x}{\partial u_l} \left(\frac{\partial^2 f_i^x}{\partial x \partial x} + \frac{\partial^2 f_i^y}{\partial y \partial x} + \frac{\partial^2 f_i^z}{\partial z \partial x} \right) - \sum_{l=1}^m \sum_{p=1}^m \frac{\partial^2 f_i^x}{\partial u_l \partial u_p} \frac{\partial u_l}{\partial x} \left(\frac{\partial f_i^x}{\partial x} + \frac{\partial f_i^y}{\partial y} + \frac{\partial f_i^z}{\partial z} \right). \end{aligned}$$

This procedure can also be applied to the other terms in the relation in Eq. (10).

For the third-order derivatives of u_i involving first-order time differentiation, we assume that the following equations are valid:

$$\begin{aligned} \frac{\partial^3 u_i}{\partial x \partial \Psi \partial t} &= -\frac{\partial}{\partial \Psi} \left(\frac{\partial^2 f_i^x}{\partial x \partial x} + \frac{\partial^2 f_i^y}{\partial y \partial x} + \frac{\partial^2 f_i^z}{\partial z \partial x} \right), \\ \frac{\partial^3 u_i}{\partial y \partial \Psi \partial t} &= -\frac{\partial}{\partial \Psi} \left(\frac{\partial^2 f_i^x}{\partial x \partial y} + \frac{\partial^2 f_i^y}{\partial y \partial y} + \frac{\partial^2 f_i^z}{\partial y \partial z} \right), \\ \frac{\partial^3 u_i}{\partial z \partial \Psi \partial t} &= -\frac{\partial}{\partial \Psi} \left(\frac{\partial^2 f_i^x}{\partial x \partial z} + \frac{\partial^2 f_i^y}{\partial y \partial z} + \frac{\partial^2 f_i^z}{\partial z \partial z} \right), \\ \frac{\partial^3 u_i}{\partial t \partial t \partial t} &= -\frac{\partial}{\partial t} \left(\frac{\partial^2 f_i^x}{\partial x \partial t} + \frac{\partial^2 f_i^y}{\partial y \partial t} + \frac{\partial^2 f_i^z}{\partial z \partial t} \right), \end{aligned} \quad (11)$$

where $\Psi = (x, y, z, t)$. Equation (11) has terms with multiple temporal derivatives on the RHS which can be expressed in terms of spatial derivatives using the same approach used for Eq. (10).

Essentially, Eqs. (9-11) assume that the coefficients of Taylor series expansion for u_i and $f_i^{x,y,z}$ satisfy the additional higher-order equations, which are readily obtained by applying spatial differentiation to the Euler equations Eq. (1). The procedure is recursive and can be readily extended to higher-order derivatives of u_i .

To recap, all the first-, second-, and third-order derivatives of u_i and $f_i^{x,y,z}$ involving any order of time differentiation can always be replaced by relationship formulated in terms of spatial derivatives of u_i : This is achieved by the following steps: (i) the additional equations shown in Eqs. (9-11), (ii) Eqs. (6-8), and (iii) the chain rule as shown in Eqs. (6-8). As such, the independent variables in the fourth-order CESE method include only the conserved variables u_i with $i = 1, 2, \dots, m$ and their spatial derivatives. Table 1 lists the primary unknowns of the fourth-order CESE method.

Table 1: The unknowns of a three-dimensional, fourth-order CESE method.

Even-order variables	Odd-order variables		
u_i	$(u_i)_x$	$(u_i)_y$	$(u_i)_z$
$(u_i)_{xx}$	$(u_i)_{xxx}$	$(u_i)_{xxy}$	$(u_i)_{xxz}$
$(u_i)_{xy}$	$(u_i)_{xyx}$	$(u_i)_{xyy}$	$(u_i)_{xyz}$
$(u_i)_{xz}$	$(u_i)_{xzx}$	$(u_i)_{xzy}$	$(u_i)_{xzz}$
$(u_i)_{yx}$	$(u_i)_{yxx}$	$(u_i)_{yxy}$	$(u_i)_{yxz}$
$(u_i)_{yy}$	$(u_i)_{yyx}$	$(u_i)_{yyy}$	$(u_i)_{yyz}$
$(u_i)_{yz}$	$(u_i)_{yzx}$	$(u_i)_{yzy}$	$(u_i)_{yzz}$
$(u_i)_{zx}$	$(u_i)_{zxx}$	$(u_i)_{zxy}$	$(u_i)_{zxz}$
$(u_i)_{zy}$	$(u_i)_{zyx}$	$(u_i)_{zyy}$	$(u_i)_{zyz}$
$(u_i)_{zz}$	$(u_i)_{zzx}$	$(u_i)_{zzy}$	$(u_i)_{zzz}$

II.D. Space-Time Flux Conservation

In this section, the procedure of integration for space-time flux conservation is illustrated. The space-time integration is used to calculate the conserved variables and their even derivatives. Furthermore, the method presented in this section is applicable to any even derivative. As a reminder the integration is carried out in four dimensions, three space and one time. To visualize the volume in which the integration takes place it is easiest to think of it as a cube where each surface is really a volume. This volume has sides and as well as a top and bottom region. To more easily present the integration it will be split up into two parts with the first being the “side” hyperplanes and the second being the “top and bottom” hyperplanes. A hyperplane is a generic term for any shape with $n-1$ dimensions that can split an n dimensional object. In two-dimensions a hyperplane would be a line and in three-dimensions a hyperplane would be a surface.

The flux through the side and bottom faces are calculated from the known solution at the previous time step at neighboring points of the current solution point. Therefore, the calculation for fluxes through side and bottom surfaces are explicit. The flux through the top surface is a function of the solution at the new time step.

Flux through Side Hyperplane

Figure 1 shows part of the side hyperplane. For a tetrahedral mesh there would be 6 of these hyperplanes in one BCE giving a total of 24 side hyperplanes for the entire CE. The points P_i , $i = 1, 2, 3$ are at the current time step while points P'_i , $i = 1, 2, 3$ are at the next time step. Point P_i and P'_i have the same spatial coordinates but different temporal location.

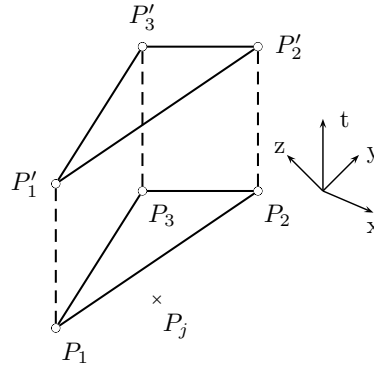


Fig. 1: The side face associated with a solution point

To evaluate the integral in Eq. (2) we calculate the normal via

$$\begin{vmatrix} \hat{i} & \hat{j} & \hat{k} & \hat{t} \\ x_2 - x_1 & y_2 - y_1 & z_2 - z_1 & t_2 - t_1 \\ x_3 - x_1 & y_3 - y_1 & z_3 - z_1 & t_3 - t_1 \\ x'_1 - x_1 & y'_1 - y_1 & z'_1 - z_1 & t'_1 - t_1 \end{vmatrix} = [N^x \hat{i}, N^y \hat{j}, N^z \hat{k}, 0 \hat{t}] \quad (12)$$

By applying Eq. (12) to Eq. (2) yields:

$$\sum_{x^i, y, z} \sum_{a=0}^N \sum_{b=0}^{N-a} \sum_{c=0}^{N-a-b} \sum_{d=0}^{N-a-b-c} \frac{\partial f_i^{x^i}}{\partial x^a \partial y^b \partial z^c \partial t^d} \frac{n_{x^i}}{a!b!c!d!} \int_{V_S^{4D}} (x - x_j)^a (y - y_j)^b (z - z_j)^c (t - t^n)^d dV_S^4, \quad (13)$$

where V_S^{4D} represents the integration over the side hyperplane. This is the integration will have to be repeated for each BCE. By noticing that the temporal integration is decoupled from the spatial integration we can integrate the temporal terms separately. We can also represent the volume through a parametric equation with two independent variables, e.g. $x = x_1 + (x_2 - x_1)u + (x_3 - x_1)v$. This leads to the equation,

$$\begin{aligned} \sum_{x^i, y, z} \sum_{a=0}^N \sum_{b=0}^{N-a} \sum_{c=0}^{N-a-b} \sum_{d=0}^{N-a-b-c} \frac{\partial f_i^{x^i}}{\partial x^a \partial y^b \partial z^c \partial t^d} \frac{N_{x^i}^{(3)}}{a!b!c!(d+1)!} \left(\frac{\Delta t}{2} \right)^{d+1} \int_0^1 \int_0^{1-u} [(x_2 - x_1)u + (x_3 - x_1)v + x_1 - x_j]^a \\ [(y_2 - y_1)u + (y_3 - y_1)v + y_1 - y_j]^b [(z_2 - z_1)u + (z_3 - z_1)v + z_1 - z_j]^c dvdu, \end{aligned} \quad (14)$$

where

$$\hat{N}^{(3)} = \begin{vmatrix} \hat{i} & \hat{j} & \hat{k} \\ x_2 - x_1 & y_2 - y_1 & z_2 - z_1 \\ x_3 - x_1 & y_3 - y_1 & z_3 - z_1 \end{vmatrix} \quad (15)$$

The integral in Eq. (14) will be integrated for select combinations of a, b and c in Appendix A.

Flux through the Top and Bottom Hyperplane

To proceed, we present the calculation of the flux through the bottom hyperplane of the CE centered at point P_i . The bottom hyperplane of the CE is located in the preceding time step $n - 1/2$. The calculation of the flux through the bottom hyperplane of the CE requires integration over four triangular bipyramids. A triangular bipyramid is a three-dimensional object consisting of two tetrahedrons that share a common face. Figure 2 is a diagram of a portion of the top and bottom hyperplane. This shape is called a triangular bipyramid which is composed of two tetrahedrons that share a common face. In this figure the common face is shown in red while the blue edges makes up the tetrahedron associated with the neighboring cell and the black edges are associated with the central cell. The point P_i is the current solution point, point P_4 is the neighboring cell center and the point P_j is the neighboring solution point. When integrating over the bottom hyperplane the Taylor series is expanded from P_j but when integrating over the top hyperplane the Taylor series is expanded from P_i . Since the geometry of the top and bottom hyperplanes is the same only the derivation for the bottom hyperplane will be detailed.

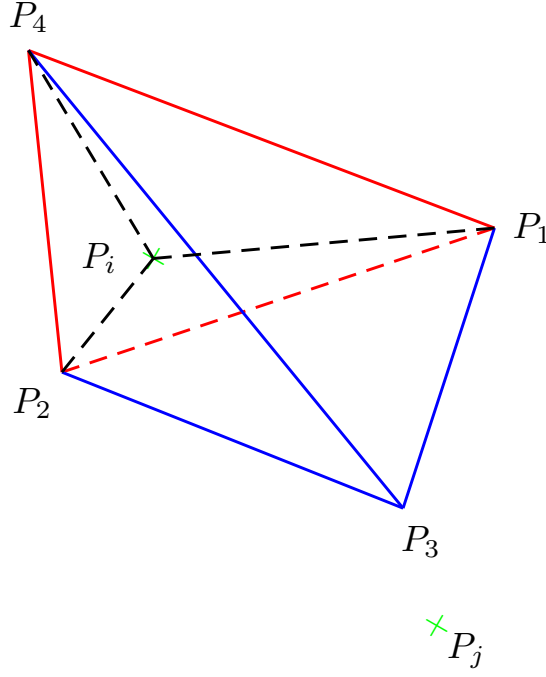


Fig. 2: The bottom and top hyperplane

To evaluate the integral in Eq. (2) over the bottom and top hyperplane we need the normal which is

$$\hat{N} = \begin{vmatrix} \hat{i} & \hat{j} & \hat{k} & \hat{t} \\ x_2 - x_1 & y_2 - y_1 & z_2 - z_1 & t_2 - t_1 \\ x_3 - x_1 & y_3 - y_1 & z_3 - z_1 & t_3 - t_1 \\ x_4 - x_1 & y_4 - y_1 & z_4 - z_1 & t_4 - t_1 \end{vmatrix} = - \begin{vmatrix} x_2 - x_1 & y_2 - y_1 & z_2 - z_1 \\ x_3 - x_1 & y_3 - y_1 & z_3 - z_1 \\ x_4 - x_1 & y_4 - y_1 & z_4 - z_1 \end{vmatrix} \hat{t}. \quad (16)$$

It should be noted that the normals in the i, j and k direction are all zero. Applying Eq. (16) to Eq. (2) yields:

$$\sum_{a=0}^N \sum_{b=0}^{N-a} \sum_{c=0}^{N-a-b} \frac{\partial^{a+b+c} u_i}{\partial x^a \partial y^b \partial z^c} \frac{n^t}{a!b!c!} \int_{V_B^{4D}} (x - x_j)^a (y - y_j)^b (z - z_j)^c dV_B^{4D}, \quad (17)$$

where n^t is the normal component in the t direction. It should be noted that there is no time integration in Eq. (17) because all points inside of the volume V_B^{4D} are at the same time step. To integrate Eq. (17) we represent the volume into its parametric form. After applying the parametric transformation Eq (17) becomes

$$\sum_{a=0}^N \sum_{b=0}^{N-a} \sum_{c=0}^{N-a-b} \frac{\partial^{a+b+c} u_i}{\partial x^a \partial y^b \partial z^c} \frac{|J|n^t}{a!b!c!} \int_0^1 \int_0^{1-u} \int_0^{1-u-v} \left([(x_2 - x_1)u + (x_3 - x_1)v + (x_4 - x_1)w + x_1 - x_j]^a \right. \\ \left. [(y_2 - y_1)u + (y_3 - y_1)v + (y_4 - y_1)w + y_1 - y_j]^b [(z_2 - z_1)u + (z_3 - z_1)v + (z_4 - z_1)w + z_1 - z_j]^c \right) dw dv du \quad (18)$$

where $|J| = \det(\hat{N})$. This leads to the simplification of $|J|n^t = N^t$. The integral in Eq. (18) will be integrated for select combinations of a, b and c in Appendix B.

To progress an even derivative to the next time step we need to apply either Eq. (18) or Eq. (14) to each hyperplane in every BCE associated with the current cell (j, n) and then take the sum of all integrations. For a tetrahedral mesh each cell has four BCEs and each BCE has three “side” hyperplanes, one “top” hyperplane and one “bottom” hyperplane.

II.E. First Derivatives

In this section we detail the procedure used to calculate the first derivatives of the conserved variables. The method used is very similar to the one used in the second-order scheme, the major difference is that a third-order Taylor series is used instead of a first-order Taylor series. A brief outline used to calculate the first derivatives is detailed below, for a complete derivation please see a second-order derivation.^{7,8} As a reminder the superscript and subscripts on the outside of a bracket represent the location where the Taylor series coefficients are calculated at.

As a preface we will lay out the necessary geometry. First consider the current cell at location j_0 and the surrounding cells denoted by j_r for $r = 1, 2, \dots, N_b$, where N_b is the number of neighbors. For a tetrahedral mesh N_b would be 4. These cells exist at both the current time step, n , and the previous time step $n - 1/2$ giving them the space-time location of (j_r, n) $r = 0, \dots, N_b$ for the current time step and $(j_r, n - 1/2)$ $r = 0, \dots, N_b$ for the previous time step. There are two important locations in each cell, (i) the centroid denoted by j_r^\times , (ii) the Taylor expansion point denoted by j_r^+ . The derivation below is applicable to any type of mesh, i.e. tetrahedral, hexagonal, prism, and four-sided pyramid, but for simplicity we will restrict our examples to tetrahedral meshes. In what follows is an outline detailing each step required to calculate the first derivatives.

1. Determine the location of the Taylor series expansion points using either the c - τ scheme detailed in⁸ or the edge based derivative (EBD) scheme.⁹
2. Perform Taylor series expansions from (j_0^\times, n) to each (j_r^+, n) $r = 1, \dots, N_b$.

$$[u_i^*(j_r^+, n)]_{j_0^\times}^n = \sum_{a=0}^A \sum_{b=0}^{A-a} \sum_{c=0}^{A-a-b} \left(\frac{\partial^{a+b+c} u_i}{\partial x^a \partial y^b \partial z^c} \right)_{j_0^\times}^n \frac{(x_{j_r^+} - x_{j_0^\times})^a (y_{j_r^+} - y_{j_0^\times})^b (z_{j_r^+} - z_{j_0^\times})^c}{a!b!c!}. \quad (19)$$

By applying Eq (19) to each of the surrounding cells we obtain N_b equations with three+ N_b unknowns per governing equation. The unknowns are the first derivatives of the conserved variables and the values of the conserved variables at the expansion points, $[u_i^*(j^+, n)]_{j_0^\times}^n$ $j = 1, \dots, N_b$.

3. Next the unknowns at $[u_i^*(j_r^+, n)]_{j_0^\times}^n$ are approximated by a Taylor series expansion from j_r^\times at the previous half time step to j_r^+ at the current time step, i.e. $[u_i^*(j_r^+, n)]_{j_0^\times}^n \approx [u_i'(j_r^+, n)]_{j_r^\times}^{n-1/2}$ where

$$[u_i'(j^+, n)]_{j_r^\times}^{n-1/2} = \sum_{a=0}^A \sum_{b=0}^{A-a} \sum_{c=0}^{A-a-b} \sum_{d=0}^{A-a-b-c} \left(\frac{\partial^{a+b+c+d} u_i}{\partial x^a \partial y^b \partial z^c \partial t^d} \right)_{j_r^\times}^{n-1/2} \frac{(x_{j_r^+} - x_{j_r^\times})^a (y_{j_r^+} - y_{j_r^\times})^b (z_{j_r^+} - z_{j_r^\times})^c \left(\frac{\Delta t}{2} \right)^d}{a!b!c!d!} \quad (20)$$

By substituting Eq. (20) into Eq. (19) and moving the unknowns to the LHS we get

$$[(u_i)_x]_{j_0^\times}^n \Delta x_{j_r^+} + [(u_i)_y]_{j_0^\times}^n \Delta y_{j_r^+} + [(u_i)_z]_{j_0^\times}^n \Delta z_{j_r^+} = [u_i'(j^+, n)]_{j_r^\times}^{n-1/2} - \sum_{a=0}^A \sum_{b=0}^{A-a} \sum_{c=0}^{A-a-b} \left(\frac{\partial^{a+b+c} u_i}{\partial x^a \partial y^b \partial z^c} \right)_{j_0^\times}^n \frac{(\Delta x_{j_r^+})^a (\Delta y_{j_r^+})^b (\Delta z_{j_r^+})^c}{a!b!c!}, \quad (21)$$

where $\Delta x_{j_r^+} = x_{j_r^+} - x_{j_0^\times}$, $\Delta y_{j_r^+} = y_{j_r^+} - y_{j_0^\times}$, $\Delta z_{j_r^+} = z_{j_r^+} - z_{j_0^\times}$ and $(a, b, c) \neq (1, 0, 0), (0, 1, 0), (0, 0, 1)$.

4. By applying Eq. (21) to neighboring cells we have now have three unknowns and N_b equations which leads to an overdetermined system. This is actually advantageous because it allows us to determine

multiple solutions and then select the most appropriate solution. The possible solutions are determined by grouping Eqs. (21) is sets of three to generate a potential solution. For example a tetrahedral mesh has four surrounding cells and would be grouped as $[(1, 2, 3), (1, 2, 4), (2, 3, 4)]$. Taking the first triplet from the set would result in the following equation:

$$\begin{bmatrix} \Delta x_{1+} & \Delta y_{1+} & \Delta z_{1+} \\ \Delta x_{2+} & \Delta y_{2+} & \Delta z_{2+} \\ \Delta x_{3+} & \Delta y_{3+} & \Delta z_{3+} \end{bmatrix} \begin{bmatrix} (u_i)_x^{(1)} \\ (u_i)_y^{(1)} \\ (u_i)_z^{(1)} \end{bmatrix} = \begin{bmatrix} [u'_i(1^+, n)]_{1 \times}^{n-1/2} - \sum_{a=0}^A \sum_{b=0}^{A-a} \sum_{c=0}^{A-a-b} \left(\frac{\partial^{a+b+c} u_i}{\partial x^a \partial y^b \partial z^c} \right)_{j_0^\times}^n \frac{(\Delta x_{1+})^a (\Delta y_{1+})^b (\Delta z_{1+})^c}{a!b!c!} \\ [u'_i(2^+, n)]_{2 \times}^{n-1/2} - \sum_{a=0}^A \sum_{b=0}^{A-a} \sum_{c=0}^{A-a-b} \left(\frac{\partial^{a+b+c} u_i}{\partial x^a \partial y^b \partial z^c} \right)_{j_0^\times}^n \frac{(\Delta x_{2+})^a (\Delta y_{2+})^b (\Delta z_{2+})^c}{a!b!c!} \\ [u'_i(3^+, n)]_{3 \times}^{n-1/2} - \sum_{a=0}^A \sum_{b=0}^{A-a} \sum_{c=0}^{A-a-b} \left(\frac{\partial^{a+b+c} u_i}{\partial x^a \partial y^b \partial z^c} \right)_{j_0^\times}^n \frac{(\Delta x_{3+})^a (\Delta y_{3+})^b (\Delta z_{3+})^c}{a!b!c!} \end{bmatrix} \quad (22)$$

for $(a, b, c) \neq (0, 1, 0), (1, 0, 0), (0, 0, 1)$.

Using Eq (22) on all of systems of equations will generate multiple solutions to $(u_i)_x$, $(u_i)_y$ and $(u_i)_z$. The superscript (1) for the unknowns in Eq (22) represents the first possible solution for $(u_i)_x$, $(u_i)_y$ and $(u_i)_z$.

5. The final step is to weight the possible solutions together to get the optimum solution. Any of the previously derived weighting schemes are applicable to the higher order CESE method with out requiring any changes. In the present investigation the W2⁸ and S2¹⁰ schemes are used.

II.F. Order of Calculation

In this subsection we list the order in which each derivatives is calculated. Since both the even and odd derivatives requires information from the current time step the order in which the various derivatives are updated is important to ensure that the procedure is explicit. We will limit this procedure to a fourth-order scheme but the this method can be easily expanded to sixth-, eighth- or even higher orders of accuracy. For a fourth-order scheme this is the order in which the values are calculated.

1. Temporal derivatives of the conserved variables and the fluxes and their spatial and temporal derivatives.
2. Second derivatives, e.g. $(u_i)_{xx}, (u_i)_{xy}, (u_i)_{xz}$
3. Third derivatives, e.g. $(u_i)_{xxx}, (u_i)_{xxy}, (u_i)_{xxz}$
4. Conserved variables, u_i
5. First derivatives, $(u_i)_x, (u_i)_y, (u_i)_z$.

Second Derivatives

To proceed, we apply all possible second derivatives with repetition to Eq. (1) to yield the following additional equations:

$$\nabla \cdot \frac{\partial^2 \mathbf{h}_i}{\partial \Psi_1 \partial \Psi_2} = 0, \quad (\Psi_1, \Psi_2) = \{(x, x), (x, y), (x, z), (y, x), (y, y), (y, z), (z, x), (z, y), (z, z)\}.$$

Recall that $\mathbf{h} = (f_i^x, f_i^y, f_i^z, u_i)$ is the space-time flux vector. Aided by the Gauss theorem in the three-dimensional space-time domain, the above differential equations are recast into the following integral equations:

$$\oint \frac{\partial^2 \mathbf{h}_i}{\partial \Psi_1 \partial \Psi_2} \cdot d\mathbf{s} = 0 \quad (\Psi_1, \Psi_2) = \{(x, x), (x, y), (x, z), (y, x), (y, y), (y, z), (z, x), (z, y), (z, z)\}. \quad (23)$$

In the setting of the fourth-order CESE method, $(u_i)_{xx}$ is represented by using the first-order Taylor series expansion with $(u_i)_{txx}$, $(u_i)_{xxx}$, and $(u_i)_{yxx}$ as the coefficients. The integration can be straightforwardly performed based on the original second-order CESE method. Essentially, we invoke the original CESE nine times to calculate the second order spatial derivatives at the solution point (j, n) .

Third Derivatives

Once the second-derivatives are calculated, the third-derivatives of u_i listed in Table 1 are calculated by central-differencing the second derivatives of u_i . By slightly modifying the procedure outline in Section II.E we obtain the third derivatives. For example to determine $(u_i)_{xyx}$, $(u_i)_{xyy}$, $(u_i)_{xyz}$ we would obtain

$$\begin{bmatrix} \Delta x_{1+} & \Delta y_{1+} & \Delta z_{1+} \\ \Delta x_{2+} & \Delta y_{2+} & \Delta z_{2+} \\ \Delta x_{3+} & \Delta y_{3+} & \Delta z_{3+} \end{bmatrix} \begin{bmatrix} (u_i)_{xyx}^{(1)} \\ (u_i)_{xyy}^{(1)} \\ (u_i)_{xyz}^{(1)} \end{bmatrix} = \begin{bmatrix} [(u'_i)_{xy}(1^+, n)]_{1 \times}^{n-1/2} - \sum_{a=0}^A \sum_{b=0}^{A-a} \sum_{c=0}^{A-a-b} \left(\frac{\partial^{a+b+c} u_i}{\partial x^a \partial y^b \partial z^c} \right)_{j_0^\times}^n \frac{(\Delta x_{1+})^a (\Delta y_{1+})^b (\Delta z_{1+})^c}{a!b!c!} \\ [(u'_i)_{xy}(2^+, n)]_{2 \times}^{n-1/2} - \sum_{a=0}^A \sum_{b=0}^{A-a} \sum_{c=0}^{A-a-b} \left(\frac{\partial^{a+b+c} u_i}{\partial x^a \partial y^b \partial z^c} \right)_{j_0^\times}^n \frac{(\Delta x_{2+})^a (\Delta y_{2+})^b (\Delta z_{2+})^c}{a!b!c!} \\ [(u'_i)_{xy}(3^+, n)]_{3 \times}^{n-1/2} - \sum_{a=0}^A \sum_{b=0}^{A-a} \sum_{c=0}^{A-a-b} \left(\frac{\partial^{a+b+c} u_i}{\partial x^a \partial y^b \partial z^c} \right)_{j_0^\times}^n \frac{(\Delta x_{3+})^a (\Delta y_{3+})^b (\Delta z_{3+})^c}{a!b!c!} \end{bmatrix}$$

for $(a, b, c) \neq (0, 1, 0), (1, 0, 0), (0, 0, 1)$.

Which simplifies to

$$\begin{bmatrix} \Delta x_{1+} & \Delta y_{1+} & \Delta z_{1+} \\ \Delta x_{2+} & \Delta y_{2+} & \Delta z_{2+} \\ \Delta x_{3+} & \Delta y_{3+} & \Delta z_{3+} \end{bmatrix} \begin{bmatrix} (u_i)_{xyx}^{(1)} \\ (u_i)_{xyy}^{(1)} \\ (u_i)_{xyz}^{(1)} \end{bmatrix} = \begin{bmatrix} [(u'_i)_{xy}(1^+, n)]_{1 \times}^{n-1/2} - [(u_i)_{xy}]_{j_0^\times}^n \\ [(u'_i)_{xy}(2^+, n)]_{2 \times}^{n-1/2} - [(u_i)_{xy}]_{j_0^\times}^n \\ [(u'_i)_{xy}(3^+, n)]_{3 \times}^{n-1/2} - [(u_i)_{xy}]_{j_0^\times}^n \end{bmatrix} \quad (24)$$

Eq. (24) is nearly identical to the equation used to determine the first derivatives in the second-order scheme. This procedure is then used to determine all other third derivatives.

Conserved Variables

The next step is to update the conserved variables, u_i . For this step you use the method outlined in Section II.D. The only modification required is to set $N = 3$ in Eqs. (14) and (18). Although the integration over the top surface uses solutions from the current time step the scheme is still explicit. This is possible because the second and third derivatives are all ready known and the integration of the first derivatives is zero. This leaves u_i as the only unknown and is easily separated. The integration of the first derivatives are zero, not the first derivatives them self.

First Derivatives

The first derivatives are calculated using the procedure listed in Section II.E.

III. Results and Discussion

To assess the accuracy of the three-dimensional, unstructured hyperbolic solver, we consider the following benchmark problems: (i) the advection equation to assess the convergence rate, and (ii) the Euler equation to simulate supersonic flow over a spherical blunt body.

III.A. Advection Equation for Convergence

The advection equation, Eq. (25), is used to verify the order convergence of the new scheme.

$$\frac{\partial u}{\partial t} + a_x \frac{\partial u}{\partial x} + a_y \frac{\partial u}{\partial y} + a_z \frac{\partial u}{\partial z} = 0 \quad (25)$$

A solution is assumed to take the form

$$u = \sin(a_x x + a_y y + a_z z + a_t t), \quad (26)$$

the domain is a cube of length 2π and periodic boundary conditions are imposed. Under these assumptions the wave speeds are $a_x = a_y = a_z = 1$ and $a_t = -(a_x^2 + a_y^2 + a_z^2)$. The simulation is allowed to run for a non-dimensional time of 25 which allows the wave to progress through the domain $25/(2\pi)$ times. To determine the rate of convergence the L2 norm is calculated and compared against a characteristic length. The characteristic length is taken to be $(Volume/ncell)^{-1/3}$, where $ncell$ is the number of cells. The result of the simulation is shown in Figure 3. A best fit line was taken and the convergence rate was determined to be 4.3 and 2.6 for the fourth and second-order schemes respectively.

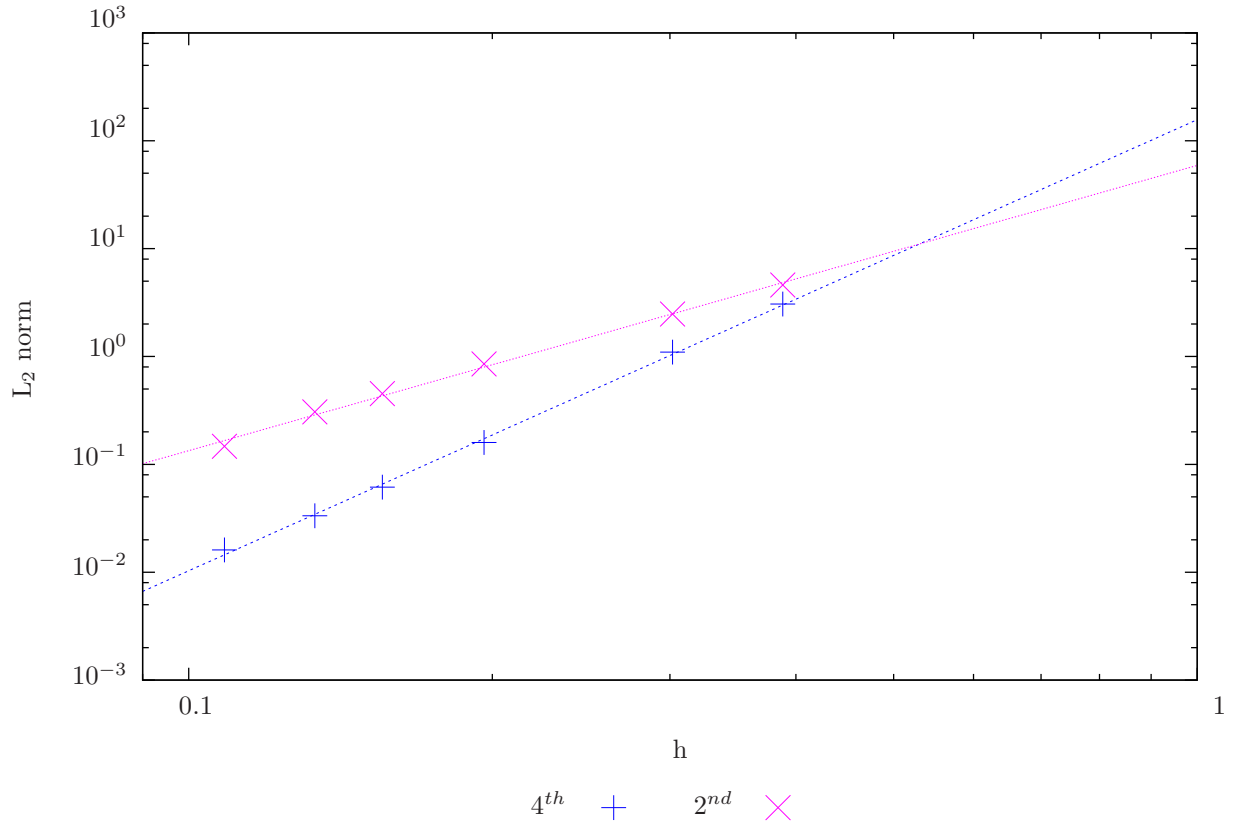


Fig. 3: Convergence test for the 3D convection equation

III.B. Supersonic Flow over a Blunt Body

To determine the schemes capability to resolve discontinuities supersonic flow over a sphere is considered. The properties of interest are the post shock density, shock standoff distance and the shock profile. For the simulation the working fluid is air with specific heat ratio 1.4 and a gas constant 287.15 J/kg K. The free stream Mach number, pressure and density are 3.0, 1 bar, and 1.23 kg/m³ respectively. The radius of the sphere is 0.5 meters. The simulation was run for 5 thousand iterations at an average CFL number of 0.533. The post shock density was calculated to be 4.613 kg/m³ which compares favorably to the analytical value

of 4.744 kg/m^3 . The shock standoff distance was approximated to be 0.11 which also compares favorably to the value of 0.10 predicted by Ambrosio and Wortman's¹¹ relation,

$$\Delta = 0.143R e^{3.24/M_\infty^2}, \quad (27)$$

where R is the radius of the sphere and M_∞ is the free stream Mach number.

The profile of the shock around the sphere is obtained by the relationship generated by Billig¹² and is equal to

$$x = R + \Delta - R_c \cot^2 \theta \left[\left(1 + \frac{y^2 \tan^2 \theta}{R_c^2} \right)^{0.5} - 1 \right], \quad (28)$$

where Δ is the shock stand off distance given by Eq. (27), θ is the Mach angle is equal to $\sin^{-1}(1/M_\infty)$ and R_c is the radius of curvature and is equal to

$$R_c = 1.143R e^{(0.54/(M_\infty-1))^{1.2}}.$$

A numerical Schlieren image is shown in Figure 4. This figure shows the shock profile generated by the simulation and the points represent shock profile generated by Eq. (28). The shock profile predicted by Eq. (28) agrees favorably with the numerical results.

IV. Concluding Remarks

This paper details the derivation and validation of a new fourth-order CESE method used to solve three-dimensional hyperbolic PDEs on unstructured tetrahedral meshes. The formulation was found to retain all favorable features of the original second-order CESE method, including (i) the use of the most compact mesh stencil involving only the immediate neighboring nodes of the central node where the unknowns are sought, (ii) the stability constraint of the four-order CESE method remains to be $\text{CFL} \leq 1$, and (iii) completely explicit operation in the time marching calculation. To demonstrate the capabilities of the new method, two test cases were reported: (i) a sinusoidal wave modeled by the advection equation, used to confirm higher-order convergence (ii) Mach 3 air flow around a spherical blunt body used to determine the schemes ability to accurately resolve discontinuities. Future work will investigate the effects of various re-weighting schemes on the accuracy of the results and the development of a three-dimensional Navier-Stokes solver.

A. Side Integration

This section will list selected integrations for the integral in Eq. (14). To start we will define $\Delta x_i = x_i - x_j$, $\Delta y_i = y_i - y_j$, $\Delta z_i = z_i - z_j$ for $i = 1, 2, 3$. With this definition Eq. (14) becomes

$$\mathcal{L}_{a,b,c}^s = \int_0^1 \int_0^{1-u} \prod_{j=1}^3 \left[\Delta \Psi_2^j u + \Delta \Psi_3^j v + \Delta \Psi_1^j (1-u-v) \right]^{\omega_j} dv du,$$

where $\Psi = \{x, y, z\}$ and $\omega = \{a, b, c\}$.

When $a = 1$ and $b = c = 0$ the integration is

$$\mathcal{L}_{1,0,0}^s = \frac{1}{6} \sum_{i=1}^3 \Delta x_i.$$

When $a = b = 1$ and $c = 0$

$$\mathcal{L}_{1,1,0}^s = \frac{1}{24} \left[\sum_{i=1}^3 (\Delta x_i \Delta y_i) + \sum_{i=1}^3 \Delta x_i \sum_{i=1}^3 \Delta y_i \right].$$

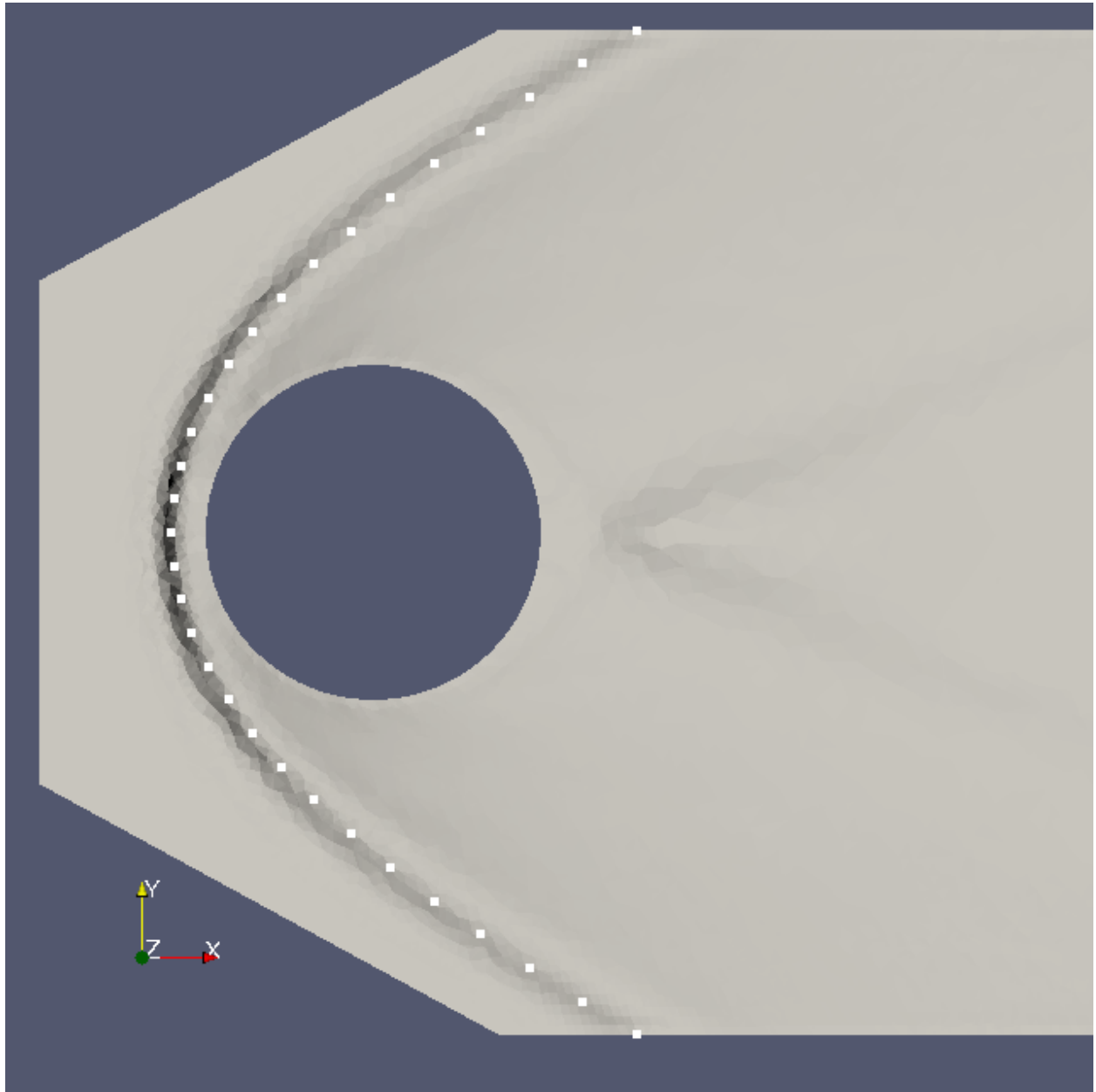


Fig. 4: Convergence test for the 3D convection equation

When $a = b = c = 1$

$$\mathcal{L}_{1,1,1}^s = \frac{1}{120} \left[\sum_{i=1}^3 \Delta x_i \sum_{i=1}^3 \Delta y_i \sum_{i=1}^3 \Delta z_i + 2 \sum_{i=1}^3 (\Delta x_i \Delta y_i \Delta z_i) + \sum_{i=1}^3 (\Delta x_i \Delta y_i) \sum_{i=1}^3 \Delta z_i + \sum_{i=1}^3 (\Delta x_i \Delta z_i) \sum_{i=1}^3 \Delta y_i + \sum_{i=1}^3 (\Delta y_i \Delta z_i) \sum_{i=1}^3 \Delta x_i \right].$$

Given these three formulas it is possible to easily derive all other integrals for a fourth-order scheme. For example to obtain the formulation for $\mathcal{L}_{2,0,0}^s$ one may substitute Δx_i for Δy_i in the formulation for $\mathcal{L}_{1,1,0}^s$.

B. Bottom and Top Integration

This section will list selected integrations for the integral in Eq. (18). To start we will define $\Delta x_i = x_i - x_j$, $\Delta y_i = y_i - y_j$, $\Delta z_i = z_i - z_j$ for $i = 1, 2, 3$. With this definition Eq. (18) becomes

$$\mathcal{L}_{a,b,c}^{bt} = \int_0^1 \int_0^{1-u} \int_0^{1-u-v} \prod_{j=1}^3 \left[\Delta \Psi_2^j u + \Delta \Psi_3^j v + \Delta \Psi_4^j w + \Delta \Psi_1^j (1 - u - v - w) \right]^{\omega_j} dw dv du,$$

where $\Psi = \{x, y, z\}$ and $\omega = \{a, b, c\}$.

When $a = 1$ and $b = c = 0$ the integration is

$$\mathcal{L}_{1,0,0}^{bt} = \frac{1}{24} \sum_{i=1}^4 \Delta x_i.$$

When $a = b = 1$ and $c = 0$

$$\mathcal{L}_{1,1,0}^{bt} = \frac{1}{120} \left[\sum_{i=1}^4 (\Delta x_i \Delta y_i) + \sum_{i=1}^4 \Delta x_i \sum_{i=1}^4 \Delta y_i \right].$$

When $a = b = c = 1$

$$\mathcal{L}_{1,1,1}^{bt} = \frac{1}{720} \left[\sum_{i=1}^4 \Delta x_i \sum_{i=1}^4 \Delta y_i \sum_{i=1}^4 \Delta z_i + 2 \sum_{i=1}^4 (\Delta x_i \Delta y_i \Delta z_i) + \sum_{i=1}^4 (\Delta x_i \Delta y_i) \sum_{i=1}^4 \Delta z_i + \sum_{i=1}^4 (\Delta x_i \Delta z_i) \sum_{i=1}^4 \Delta y_i + \sum_{i=1}^4 (\Delta y_i \Delta z_i) \sum_{i=1}^4 \Delta x_i \right].$$

As with the derivation in Appendix A the other integrals required for a fourth-order scheme are easily obtained through substituting. For example $\mathcal{L}_{0,1,2}^{bt}$ is obtained by substituting Δz_i for Δx_i in the formulation of $\mathcal{L}_{1,1,1}^{bt}$.

References

- ¹Chang, S.-C., “A New Approach for Constructing Highly Stable High Order CESE Schemes,” *48th AIAA Aerospace Science Meeting*, Vol. 2010-543, AIAA, Orlando, FL, Jan. 2010.
- ²Bilyeu, D., Chen, Y.-Y., and Yu, S.-T. J., “High-Order CESE Methods for the Euler Equations,” *49th AIAA Aerospace Sciences Meeting*, Vol. 2011-1065, AIAA, Orlando, Florida, Jan. 2011.
- ³Bilyeu, D., Chen, Y., and Yu, S., “A Generic 4th Order 2D Unstructured Euler Solver for the CESE Method,” AIAA, Nashville, Tn, Jan. 2012.
- ⁴Dyson, R. W., “Technique for very high order nonlinear simulation and validation,” *2001.*, 2001.
- ⁵Dumbser, M. and Munz, C.-D., “Building Blocks for Arbitrary High Order Discontinuous Galerkin Schemes,” *Journal of Scientific Computing*, Vol. 27, No. 1-3, Dec. 2005, pp. 215–230.
- ⁶Chen, Y.-Y., *A Multi-Physics Software Framework on Hybrid Parallel Computing For High-Fidelity Solutions of Conservation Laws*, PhD, The Ohio State University, Columbus, Ohio, 2011.
- ⁷Wang, X.-Y. and Chang, S.-C., “A 2D Non-Splitting Unstructured Triangular Mesh Euler Solver Based on the Space-Time Conservation Element and Solution Element Method,” *Computational Fluid Dynamics JOURNAL*, Vol. 8, No. 2, 1999, pp. 309–325.
- ⁸Chang, S.-C. and Wang, X.-Y., “Multi-Dimensional Courant Number Insensitive CE/SE Euler Solvers for Applications Involving Highly Nonuniform Meshes,” *39th AIAA/ASME/SAE/ASEE Joint Propulsion Conference and Exhibit*, Huntsville, Alabama, July 2003.
- ⁹Chang, C.-L., “Three-Dimensional Navier-Stokes Calculations Using the Modified Space-Time CESE Method,” Cincinnati, Ohio, 2007.
- ¹⁰Zhang, M. and Yu, S. T. J., “CFL Number Insensitive CESE Schemes for the Two-Dimensional Euler Equations,” AIAA, Orlando, FL, June 2003.
- ¹¹Ambrosio, A. and Wortman, A., “Stagnation-point shock-detachment distance for flow around spheres and cylinders in air,” *J. Aerospace Sci.*, Vol. 29, No. 7, 1962, pp. 875.
- ¹²Billig, F. S., “Shock-wave shapes around spherical-and cylindrical-nosed bodies.” *Journal of Spacecraft and Rockets*, Vol. 4, No. 6, 1967, pp. 822823.